Research & Reviews: Journal of Material Sciences e-ISSN: 2321-6212

Thyme Functionalized Polydopamine Coated ZnO Nanoparticles With Enhanced Antibacterial Activity For Biomedical Application

Parinaz Nezhad-Mokhtari[1], Nahideh Asadi[1], Yaeghob Sharifi[2*], Morteza Milani[3]

[1]Department of Medical Nanotechnology, Tabriz University of Medical Sciences, Tabriz, Iran

[2]Department of Microbiology, Urmia University of Medical Sciences, Urmia, Iran

[3] Infectious and Tropical Diseases Research Center, Tabriz University of Medical Sciences, Tabriz, Iran

Research Article

Received: 03-Mar-2022, Manuscript No. JOMS-22-56037; **Editor assigned:** 05- Mar -2022, PreQC No. JOMS -22-56037 (PQ); **Reviewed:** 19- Mar -2022, QC No. JOMS -22-56037; **Revised:** 24- Mar -2022, Manuscript No. JOMS -22-56037 (R); **Published:** 31- Mar-2022, DOI: 10.4172/2321-6212.10.3.003.

***For Correspondence:** Yaeghob Sharifi, Department of Microbiology, Urmia University of Medical Sciences, Urmia, Iran

E-mail: ya.sharifi@gmail.com

Keywords: ZnO nanoparticles; Polydopamine; Thyme; Antibacterial agent

ABSTRACT

Bacterial infections are a major cause of injury-related death, and several efforts have been developed to deal this problem. For this goal, we were synthetized a novel antibacterial agent based on thyme functionalized polydopamine coated ZnO NPs (TH-PDA@ZnNPs). Following the synthesis of ZnO NPs, a one-step, simple method was used to surface modification of PDA@ZnNPs with TH. The finding proved that creating NPs with a rod-shaped morphology created a large surface area for bacteria to contact. The formation of a homogeneous TH layer on the surface of NPs had no substantial effect on their shape. Antibacterial assays revealed that TH-PDA@ZnNPs had a much higher antibacterial activity against *S. aureus* and *E. coli*. This shows that PDA@ZnNPs and the TH grafted on the surface of PDA@ZnNPs have an excellent synergistic antibacterial effect. In conclusion, we suggest that the prepared TH-PDA@ZnNPs could be useful as antibacterial agents for biomedical uses.

INTRODUCTION

Bacterial infections are one of the most important problems that extend the various diseases [1-4]. Although the use of antibiotics is a common means to stop bacterial activity, the increasing drug resistance is the major drawback of over prescribing and misuse of antibiotic [5-7]. Therefore, the presence of antimicrobial agents has been illustrated as an alternative approach to locally inhibit bacterial activity without side effects. Antibacterial Nanoparticles (NPs) are one of the promising agents that can limit bacterial activity [8,9]. Nanotechnology has developed various types of nanoscale materials [10]. NPs are a broad class of materials that include particulate substances that have at least

one dimension of less than 100 nm [11]. Many different types of metal NPs such as gold (Au), silver (Ag), zinc (Zn), and copper (Cu) play an important role in nanoscience and have many interesting applications, including interesting biomedical and optical uses due to their inherent antibacterial activity and brilliant colors [12]. As we know, inorganic antibacterial agents have great migration resistance, such as Ag, ZnO and Titanium Dioxide (TiO_2) NPs [13,14]. Ag NPs is the typical representative of inorganic antibacterial agents with excellent antibacterial activity [15,16]. However, its safety is controversial. Some studies indicate that Ag is toxic to the humans and environment [17]. Besides, polymer composites with Ag experience color changes owing to the Ag discoloration, which severely limits its potential uses. In addition, Ag material is costly and the Ag NPs synthesis process is complicated. ZnO is another antibacterial agent that has attracted much interest due to its low cost, high temperature resistance, antibacterial activity, photocatalysis and UV protection, color change at high temperatures, and most importantly, its safety to humans [18-20]. It is detected as a biologically safe inorganic material. Its application in cosmetic products is approved by the FDA (Food and Drug Administration) [21]. However, the disadvantage of ZnO is that its antibacterial activity is too low. Therefore, after the ZnO antibacterial activity is increased, a type of excellent antibacterial agent with excellent antibacterial activity, safety, and high temperature resistance can be acquired [22].

Surface modification of NPs with different kinds of functional groups and surface coatings are promising approaches to omit several inorganic NPs drawbacks for biomedical uses [23]. Moreover, the coatings can interact with complex biological environments and exhibit different properties depending on the application. Considering the safety and the excellent antibacterial efficacy of natural organic antibacterial agents, they are very appropriate for NPs modification to improve antibacterial activity, such as Thyme (TH) [24,25]. TH is a safe and harmless natural antibacterial and biocidal monoterpenoid agent derived from the thymus gland. It also has proper antibacterial activity against bacteria, fungi, yeast, and mold[26,27]. TH is generally recognized as a safe food additive according to the FDA [28]. Moreover, the other characteristics of TH are antifungal, antioxidant, antidiabetic, anti-inflammatory and also antitumoral alone or in combination with other compounds. In this regard, TH and Cinnamaldehyde (CA) were used in a study to modify ZnO. The antibacterial activity assays showed that TH and CA also had an excellent synergistic effect to improve the antibacterial property of ZnO-TH-CA [29]. The results also suggest that it is an effective approach to achieve a highly effective antibacterial agent by grafting both the hydrophilic TH and hydrophobic CA onto the same surface of ZnO. Dopamine (DOP) is a molecule that can mimic the bioadhesive behavior of mussels and is readily deposited on a variety of substrates by self-polymerization, resulting in Polydopamine (PDA) [30]. Due to the abundant amine and catechol groups on the surface, PDA films reportedly serve as an active template and a good reducing agent to reduce Zn ions to ZnNPs [31,32]. A suitable thickness of PDA film can inhibit Zn migration. In this content, researchers prepared PDA coated ZnO rod-shaped NPs (PDA@ZnO) with significant antibacterial activity and biocompatibility. They showed that the developed PDA@ZnO NPs were not only non-toxic to human cells, but also remarkably promoted cell survival compared to ZnO NPs. The development of reinforced active PDA@ZnO NPs using natural TH has not yet been investigated. This study aimed to prepare a novel system based on ZnO NPs and TH-PDA (TH-PDA@ZnNPs) and studying the role of TH coating on the ZnNPs antibacterial activity [33-35].

MATERIALS AND METHODS

ZnO nanoparticles (range of particle size 10-30 nm) were obtained from nanosany corporation Co. Mashhad, Iran. Dopamine hydrochloride 98% was purchased Sigma-Aldrich. Thyme powder was obtained from Tabriz, Iran. Escherichia coli ATCC 25922 and *Staphylococcus aureus* ATCC 25923 standard strains were obtained from Persian Type Culture Collection (PTCC). All other solvents and reagents were of reagent grade.

Synthesis of polydopamine functionalized ZnO NPs (PDA@ZnNPs)

PDA@ZnNPs was prepared by adding ZnO NPs to the aquas solution of dopamine [36]. Briefly, 40 mg ZnO nanoparticles was primarily washed and dispersed in deionized water by sonication. A fresh dopamine solution was prepared by dissolving of 10 mg dopamine in Tris-HCl buffer solution (pH=9) with the concentration of 2 mg/ml. Then, ZnO NPs were dispersed into dopamine solution to make a suspension. This suspension was stirred vigorously under 37°C for 24 h. Finally, PDA@ZnNPs were collected by centrifuging at 10000 rpm for 15 min and freeze-dried.

Synthesis of thyme functionalized Zn/PDA NPs (TH-PDA@ZnNPs)

The thyme solution was prepared by dissolving 100 mg thyme in absolute ethanol. TH-PDA@ZnNPs was synthesized by the same process as the PDA@ZnNPs fabrication. For this purpose, the obtained PDA@ZnNPs after the centrifuging was dispersed in ethanolic solution of thyme. This suspension was stirred vigorously under 37°C for 24 h and finally was freeze-dried.

Characterization of the synthesized nanoparticles

The chemical structure of the all the samples was evaluated by Fourier transform infrared (FTIR, Bruker, TENSOR 27, Germany) with KBr pellet in the range of 400-4000 cm^{-1}. The morphology of the obtained nanoparticles was observed by scanning electron microscopy (FE-SEM, MIRA3, Tescan). For SEM imaging, firstly, the freeze-dried samples were coated with a thin layer of gold. Also, the Energy Dispersive X-ray spectroscopy (EDX) was used to study the elements of the nanoparticles. The zeta potential of the nanoparticle's dispersion in deionized water was measured by dynamic light scattering method (ZetaSizer, Malvern Instruments, and Ver. 7.11). X-ray diffraction (XRD. Ital structure, MPD 3000) was used to analyze the structure of the nanoparticles with a 2θ range from 10° to 80° and step size of 0.001.

Antibacterial assays of nanoparticles

The antibacterial activity of the synthesized nanoparticles was assessed against *S. aureus* (Gram-positive bacteria) and *E. coli* (Gram-negative bacteria) based on the Minimum Bactericidal Concentration (MBC) and the Minimum Biofilm Eradication Concentration (MBEC).

Minimum Inhibitory Concentration (MIC) of nanoparticle

The microbroth dilution method was used to determine the minimum bactericidal concentration of nanoparticles (2019). Serial concentrations of nanoparticles were prepared in MHB (Mueller-Hinton broth) culture media (Merck, Germany). As the concentration of the nanoparticles was adjusted range from 15 to 0.029 mg/ml. A bacterial suspension equivalent to 0.5 McFarland was prepared in sterile normal saline according to the CLSI

recommendation (CLSI 2020) and inoculated into the culture medium contains nanoparticle. After 24-hour incubation at 37 °C, 100 µl of the test tubes contents were subculture on nutrient agar medium, and the growth of bacterial isolates was investigated. The MBC was defined as the lowest concentration of nanoparticle which kills 99.9% of the test strain. This experiment was conducted separately for three strains.

Minimum Biofilm Eradication Concentration (MBEC)

The Trypticase soy broth (180 µl) containing 0.5% glucose and bacterial suspension (20 µl) equal 0.5 McFarland were added to each well. After incubation overnight at 37 °C, the contents of the wells were removed and washed 3 times with 300 µl of sterile phosphate buffer. Then methanol (150 µl) was added to the wells and was incubated about for 20 min at the lab temperature. For staining, crystal violet (150 µl) was added and at ambient temperature the resultant solution was incubated for 15 min. The plates were washed and thoroughly dried by placing them upside down. Finally, acetic acid 33% (150 µl) was added to the wells and was placed 30 min at ambient temperature. The optical density of the contents of each well was detected by using a microtiter plate reader at 570 nm. According to our previous study, the cut off optical density for biofilm formation was evaluated as follow; strong formation (+++), moderate (++), weakly (+), and No Biofilm formation (0) were recorded. To optimize results and provide reliable data, the experiment was repeated triplicate per strain. Based to the above procedure, the effect of nanoparticles on biofilm eradication was investigated. With the difference that after pouring the culture medium into the wells, serial dilutions of nanoparticles were prepared in each well and bacterial suspension was added to them. Finally, the results were interpreted as follows: no biofilm formation (0); OD ≤ ODc, weak form (+); OD ≤ 2ODc, medium (++); 2ODc<OD ≤ 4OD, strong formation (+++); 4ODc<OD. The well without any nanoparticle and the other well without bacterial suspension were considered as positive and negative controls, respectively.

RESULTS AND DISCUSSION

As shown in Figure 1, the Novel TH functionalized Zn/PDA NPs (TH-PDA@ZnNPs) was successfully prepared. The morphology and shape of the obtained NPs were characterized with SEM analysis. The SEM images of the PDA@ZnNPs and TH-PDA@ZnNPs showed needle and rod-shaped NPs (Figure 2). This morphology was also detected in similar studies on the ZnO NPs synthesis using $Zn(NO_3)_2$ and $Zn(CH3COO)_2$ precursors. This morphology is favorable for several biomaterials uses due to its large surface-to volume ratio. Antibacterial features of this morphology were also illustrated in a recent study. The PDA@ZnNPs morphology after coating with thyme was not significantly altered. However, some spherical sedimentation was revealed on the NPs surface, confirming the presence of PDA/TH coating.

Figure 1. Schematic representation of steps for the synthesis of thyme functionalized Zn/PDA NPs (TH PDA@ZnNPs).

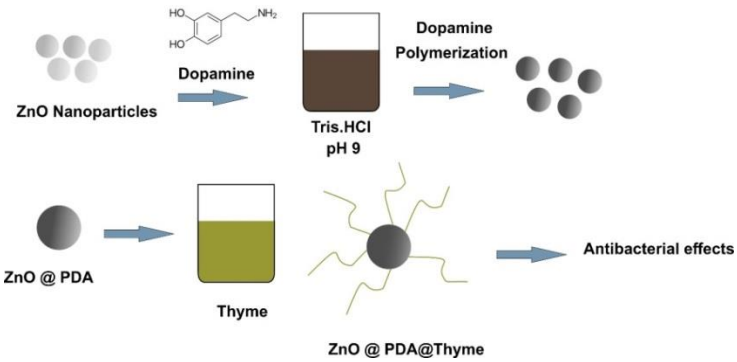

Figure 2. Scanning electron microscopy (SEM) images of polydopamine functionalized ZnO (PDA@ZnNPs (a, 200 nm), (b, 500 nm), and (c, 1 µm)) nanoparticles and thyme functionalized PDA@ZnNPs (TH-PDA@ZnNPs (d, 200 nm), (e, 500 nm), and (f, 2 µm)).

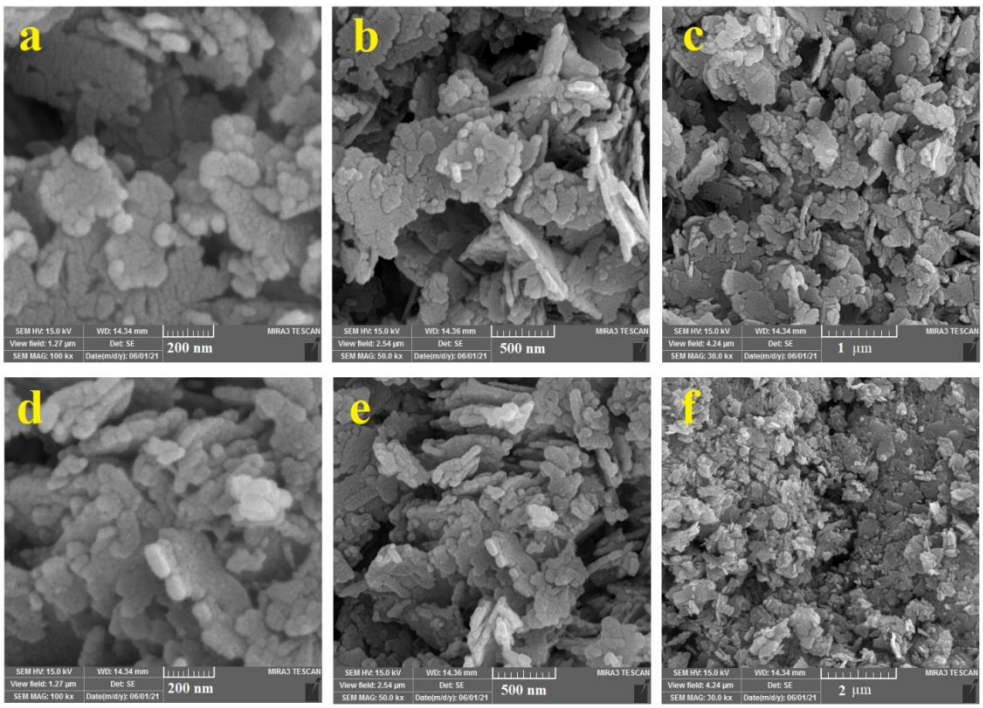

The zeta potential is an important factor for studying nanoemulsion stability. In order to find out the prepared NPs surface charge, the Zeta potential test was carried out (Figures 3 a,b). Results showed that the TH-PDA@ZnNPs (−17.2 mV) charge was negatively enhanced compared to PDA@ZnNPs (−8.36 mV). It could be realized that the electrostatic interaction between the amine groups of PDA@ZnNPs with thyme resulted in the thyme layer formation with hydroxyl functional groups leading to the creation of a negative surface charge.

Figure 3. (a) Zeta potential of polydopamine functionalized ZnO NPs (PDA@ZnNPs), (b) thyme functionalized PDA@ZnNPs (TH-PDA@ZnNPs).

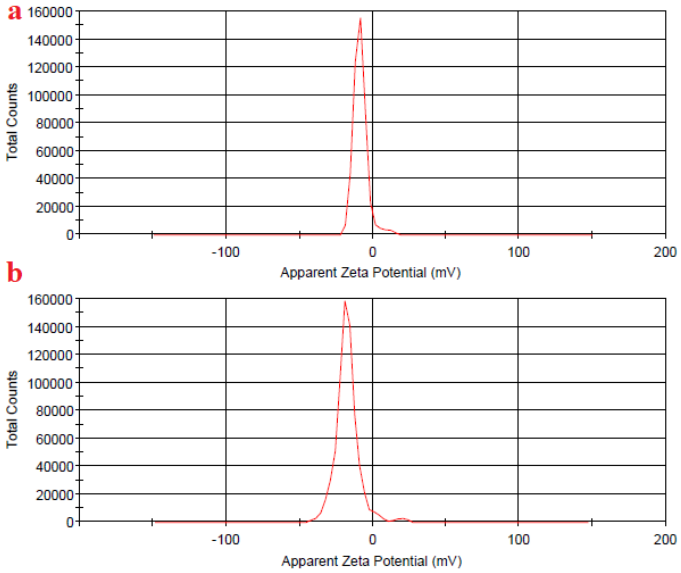

EDX analysis

The results of the EDX-dot mapping analysis for PDA@ZnNPs and TH-PDA@ZnNPs are shown in Figures 4 and 5. The presence of all applied elements, including C, N, O, and Zn, over the surface of the mentioned NPs and also the absence of any impurity were confirmed by EDX assays. The thymol adsorption group over TH-PDA@ZnNPs was also verified to be responsible for the O signal. Thymol is one of the active chemicals loaded on Zn, therefore the O signal indicates that the TH-PDA@ZnNPs were perfectly generated *via* an active, environmentally friendly reduction procedure. The sharp main peak for Zn at ~1 keV is a strong signal for the crystalline nature of biosynthesized NPs and the current work produced a consistent result in line with. Additionally, the peak intensity of each surface element and the value of the existing elements in the sample have proportionate relationships. As a result, the achieved results reveal that the prepared NPs have excellent purities and their compositions are in good accordance with the specified mass percentages, according to this statement. This observation confirms the XRD findings.

Figure 4. EDX analysis of PDA@ZnNPs.

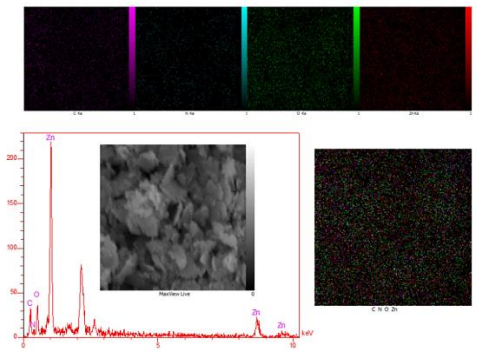

Figure 5. EDX analysis of TH-PDA@ZnNPs.

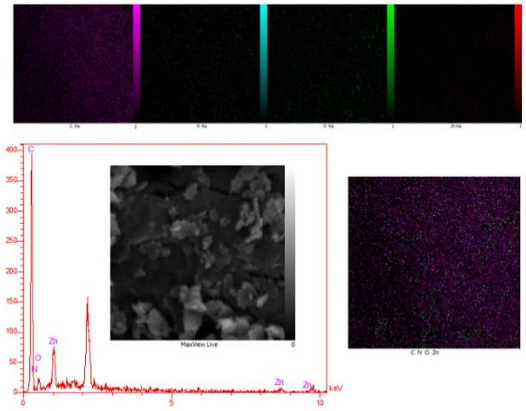

FTIR

Figure 6 indicates the FTIR spectra of crude TH, ZnO, and modified ZnNPs (PDA@ZnNPs and TH-PDA@ZnNPs). The TH spectra (Figure 6a) show an adsorption peak at ~3220 cm^{-1} corresponding to phenolic -OH stretching involving hydrogen bonding. Aromatic character of TH is indicated by C=C stretching of benzene ring at ~1615 cm^{-1}. The presence of zinc hydroxyl in the composition was demonstrated by the presence of characteristic peaks at ~1425 cm^{-1} and ~3400 cm^{-1} in the ZnO spectrum (Figure 6b). Zinc hydroxyl is an intermediate product that cannot be completely removed during the synthesis of ZnO. The spectrum of PDA@ZnNPs and TH-PDA@ZnNPs revealed that all of the characteristic peaks, as well as ZnO and TH, were present in the spectra (Figure 2). The PDA@ZnNPs spectra (Figure 6c) included a peak at 3410 cm^{-1} corresponding to the stretching vibrations of the O-H and N-H groups in the PDA. Furthermore, the peaks at ~1580 and 1250 cm^{-1} were related to C=O and C-O bonds, indicating that ZnNPs has been functionalized. The presence of PDA on ZnNPs was also confirmed by the appearance of characteristic peaks corresponding to C=N and C=C groups on the PDA@ZnO spectrum at ~1472 cm^{-1}. The spectrum of TH blended PDA@ZnNPs (Figure 6d) revealed a little shifting of position in the characteristic bands. In TH-PDA@ZnNPs spectra, the main change was detected for -OH stretching peak (~200 shifts) that might confirm interaction of TH with PDA@ZnNPs.

Figure 6. Fourier Transform Infrared (FTIR) (a) spectrum of thyme, (b) Zinc oxide nanoparticles, (c) polydopamine functionalized ZnO NPs (PDA@ZnNPs), (d) thyme functionalized PDA@ZnNPs (TH-PDA@ZnNPs).

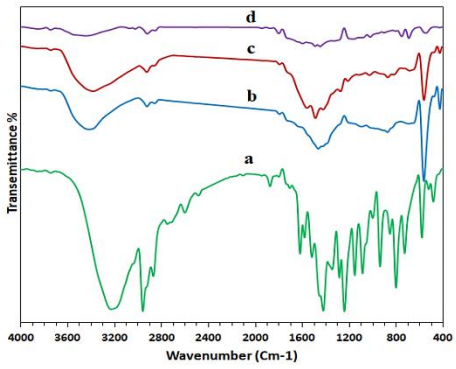

XRD analysis

The XRD patterns of ZnNPs, PDA@ZnNPs, and TH-PDA@ZnNPs showed and confirmed the crystalline nature of the NPs (Figure 7). As can be revealed from patterns, the characteristic peaks at around 2θ=31, 34, 36, 47, and 56° related to ZnO crystals [37,38]. In addition, no additional impurity peaks were found in any of the patterns. Owing to the diffraction of the PDA amorphous structure, a broad peak at 2θ=21 emerged alongside ZnO characteristic peaks after ZnO modification with PDA (PDA@ZnNPs), which is in agreement with the previous report by Tavakoli et al.[35]. In the XRD pattern of PDA@ZnNPs, the remaining peaks of $Zn(OH)_2$ were interestingly erased[39]. It can be concluded that DPA was first incorporated into $Zn(OH)_2$ and ZnNPs with free functional groups of amine and catechol, and oxidized which resulted in the $Zn(OH)_2$ conversion to ZnNPs.

Figure 7. XRD patterns of ZnNPs, PDA@ZnNPs, and TH-PDA@ZnNPs.

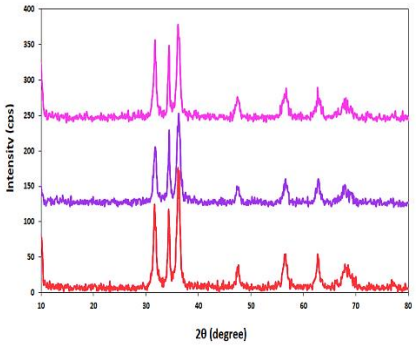

Antimicrobial Activity

Table 1 reveals the results of study the NPs samples inhibition activity against *S. aureus* and *E. coli* strains. The neat TH and PDA@ZnNPs (control) revealed weak inhibition activity against studied bacteria. Nevertheless, the Th incorporated in PDA@ZnNPs provided greater antibacterial activity. The antimicrobial property of ZnO could be ascribed to the production of Reactive Oxygen Species (ROS) by ZnO, which damages cell wall and disrupts DNA replication and protein synthesis, according to previous literature [40]. Furthermore, the Zn^{2+} ions released by ZnO increase the permeability of NPs across the bacteria cell wall, killing bacteria by interacting with cytoplasmic material [41]. The electrostatically or direct interaction between the bacterial surface and ZnO, which resulted in NP penetration in bacterial cells, is another mechanism for ZnO antibacterial activity [42]. The antibacterial activity of NPs against *S. aureus* was shown to be significantly higher than that of E. coli (see Tables 1 and 2). The bacterial cell wall system plays an important role in bacterial resistance to antibacterial drugs. The peptidoglycan layer of gram-positive bacteria is thicker than that of gram-negative bacteria [43]. However, Gram-negative bacteria have a more complicated cell wall structure, consisting of a thin peptidoglycan layer and an outer membrane with barrier features. As a result, in these bacteria outer membrane layer prevents produced ions and ROS from penetrating the bacterial cell *via* ZnO NPs.

Determination of Minimum Bactericidal Concentration (MBC): The obtained results revealed that the MBC of developed formulations compared with control groups has an excellent effect on bacteria (Table 1).

Table 1.The MBC test at different concentrations (mg/ml) of groups.

	Concentrations (µg/ml)										
Groups	Standard strains	15	7.5	3.75	1.875	0.937	0.468	0.234	0.117	0.058	0.029
PDA@ZnNPs	*E. coli*	-	-	-	-	-	-	+	+	+	+
	S. aureus	-	-	-	-	-	-	-	-	-	-
TH-PDA@ZnNPs	*E. coli*	-	-	-	-	-	-	-	-	-	-
	S. aureus	-	-	-	-	-	-	-	-	-	-
TH	*E. coli*	-	-	+	+	+	+	+	+	+	+
	S. aureus	-	-	-	+	+	+	+	+	+	+
+ : Bacterial survival; - : Not bacterial survival											

Assessment of biofilm production by different groups

The bacterial biofilm formation is a defense mechanism that protects them from antimicrobial agents, particularly antibiotics. This characteristic has a significant impact on the clinical outcome of *E. coli* and *S. aureus* infections. We assessed the production of biofilms in all of the isolates and we find that the strains were strongly positive for biofilm development. Then, in the presence of TH-loaded PDA@ZnNPs, PDA@ZnNPs, and free TH form, the minimal biofilm eradication concentration in these strains was studied. In comparison to control groups, our findings demonstrated that TH-loaded PDA@ZnNPs can eradicate biofilm formation at low concentrations (Table 2).

Table 2. Assessment of biofilm production by different groups.

Groups	Standard strains	Sub MBC concentrations (µg/ml) on MBEC					
PDA@ZnNPs	*E. coli*	234	117	58	29	14.5	7.2
		No	Weak	Weak	Weak	Moderate	Moderate
	S. aureus	14.5	7.2	3.6	1.8	0.9	0.45
		No	No	No	No	Weak	Weak
TH-PDA@ZnNPs	*E. coli*	234	117	58	29	14.5	7.2
		No	No	No	No	No	Weak
	S. aureus	14.5	7.2	3.6	1.8	0.9	0.45
		No	No	No	No	No	Weak
TH	*E. coli*	1875	937	469	234	117	58
		No	No	No	Weak	Weak	Weak
	S. aureus	1875	937	469	234	117	58
		No	No	No	No	Weak	Weak

CONCLUSION

In this study we have developed a simple approach for fabricating good antibacterial agents using Thyme (TH) functionalized polydopamine/ZnO NPs (PDA@ZnNPs). TH was grafted onto the PDA@ZnNPs successively. The antibacterial activities of the prepared NPs against *S. aureus* and *E. coli* bacteria could be notably improved by grafting TH onto the surface of PDA@ZnNPs due to the good synergistic antibacterial effect of TH and PDA@ZnNPs, according to the results of antibacterial tests. TH grafted onto the PDA@ZnNPs surface increased TH's contact probability with each bacterium, allowing them to effectively exploit their antibacterial advantages. As a result, TH-PDA@ZnNPs has a dual synergistic antibacterial effect, enhancing antibacterial activity. Besides, the developed TH-PDA@ZnNPs supposed a good potential to create blood clotting owing to its negative surface charge. The above observations not only indicated a novel approach for the development of an effective antibacterial agent that was both efficient and environmentally friendly.

Conflicts of interest

There are no conflicts to declare.

Ethics statement

The study procedure was approved by the Ethical Committee of Tabriz University of Medical Science (Approval ID:IR.TBZMED.VCR.REC.1398.303).

Acknowledgements

The authors would like to thank from the “Stem Cell Research Center, Tabriz University of medical sciences” for their kindly cooperation.

REFERENCES

1. Brachman PS, et al. Bacterial infections of humans: Epidemiology and control. 2009.
2. Dadashzadeh K, et al. Real-time PCR detection of 16S rRNA novel mutations associated with Helicobacter pylori Tetracycline resistance in Iran. Asian Pacific J Cancer Prev.2014; 15:8883-8886.
3. Coates ARM, et al. Antibiotic combination therapy against resistant bacterial infections: synergy, rejuvenation and resistance reduction. Expert Rev Anti Infect Ther. 2020; 18:5-15.
4. Hendaus MA, et al. Covid-19 induced superimposed bacterial infection. J Biomol Struct Dyn. 2020; 39:4185-4191.
5. Abroo S, et al. Methicillin-resistant Staphylococcus aureus nasal carriage between healthy students of medical and nonmedical universities. Am J Infect Control. 2017; 45:709-712.
6. Ben Y, et al. Human health risk assessment of antibiotic resistance associated with antibiotic residues in the environment: A review. Environ Res. 2019; 169:483-493.
7. Mallah N, et al. Association of knowledge and beliefs with the misuse of antibiotics in parents: A study in Beirut (Lebanon). PLoS One.2020; 15:e0232464.
8. Ojemaye MO, et al. Nanotechnology as a viable alternative for the removal of antimicrobial resistance determinants from discharged municipal effluents and associated watersheds: A review. J Environ Manage. 2020ss; 275:111234.

9. Kalelkar PP, et al. Biomaterial-based antimicrobial therapies for the treatment of bacterial infections. Nat Rev Mater. 2022;7:39-54.
10. Taran M, et al. Benefits and application of nanotechnology in environmental science: an overview. Biointerface Res Appl Chem. 2021;11:7860-7870.
11. Anselmo AC, et al. Nanoparticles in the clinic: An update. Bioeng Transl Med. 2019;4:e10143.
12. Sánchez-López E, et al. Metal-based nanoparticles as antimicrobial agents: An overview. Nanomaterials. 2020;10:292.
13. Fang M, et al. Antibacterial activities of inorganic agents on six bacteria associated with oral infections by two susceptibility tests. Int J Antimicrob Agents. 2006;27:513-517.
14. Chen R, et al. Antibacterial activity, cytotoxicity and mechanical behavior of nano-enhanced denture base resin with different kinds of inorganic antibacterial agents. Dent Mater J. 2017;36:693-699.
15. Chernousova S, et al. Silver as antibacterial agent: Ion, nanoparticle, and metal. Angew Chemie - Int Ed. 2012;52:1636-1653.
16. Hamad A, et al. Silver Nanoparticles and Silver Ions as Potential Antibacterial Agents. J Inorg Organomet Polym Mater. 2020;30:4811-4828.
17. Zhang W, et al. Chemical transformation of silver nanoparticles in aquatic environments: Mechanism, morphology and toxicity. Chemosphere. 2018;191:324-334.
18. Liu J, et al. A review on bidirectional analogies between the photocatalysis and antibacterial properties of ZnO. J Alloys Compd. 2019;783:898-918.
19. Jiang S, et al. ZnO Nanomaterials: Current Advancements in Antibacterial Mechanisms and Applications. Front. Chem. 2020;8.
20. Liu L, et al. Facile preparation PCL/ modified nano ZnO organic-inorganic composite and its application in antibacterial materials. J Polym Res. 2020;27.
21. Espitia PJP, et al. Zinc Oxide Nanoparticles for Food Packaging Applications. Antimicrobial Food Packaging .
22. Lallo da Silva B, et al. Increased antibacterial activity of ZnO nanoparticles: Influence of size and surface modification. Colloids Surfaces B Biointerfaces. 2019;177:440-447.
23. El-Naggar ME, et al. Surface modification of SiO2 coated ZnO nanoparticles for multifunctional cotton fabrics. J Colloid Interface Sci. 2017;498:413-422.
24. Shahriary M, et al. In situ green synthesis of Ag nanoparticles on herbal tea extract (Stachys lavandulifolia)-modified magnetic iron oxide nanoparticles as antibacterial agent and their 4-nitrophenol catalytic reduction activity. Mater Sci Eng C. 2018;90:57-66.
25. Alavi M, et al. Synthesis and modification of bio-derived antibacterial Ag and ZnO nanoparticles by plants, fungi, and bacteria. Drug Discov Today. 2021;26:1953-1962.
26. Marchese A, et al. Antibacterial and antifungal activities of thymol: A brief review of the literature. Food Chem. 2016;210:402-414.
27. Cai R, et al. Antibacterial activity and mechanism of thymol against Alicyclobacillus acidoterrestris vegetative cells and spores. LWT. 2019;105:377-384.
28. Zhu Z, et al. Microencapsulation of thymol in poly(lactide-co-glycolide) (PLGA): Physical and antibacterial properties. Materials (Basel). 2019;12:1133.

29. Shi Y, et al. Green cinnamaldehyde and thymol modified zinc oxide with double synergistic antibacterial effects in polypropylene. J Appl Polym Sci 138.
30. Emadoddin M, et al. An antifouling impedimetric sensor based on zinc oxide embedded polyvinyl alcohol nanoplatelets for wide range dopamine determination in the presence of high concentration ascorbic acid. J Pharm Biomed Anal. 2021;205:114278.
31. Jatoi AW, et al. Characterizations and application of CA/ZnO/AgNP composite nanofibers for sustained antibacterial properties. Mater Sci Eng C. 2019;105:110077.
32. Alipour N, et al. Chelating ZnO-dopamine on the surface of graphene oxide and its application as pH-responsive and antibacterial nanohybrid delivery agent for doxorubicin. Mater Sci Eng C. 2020;108:110459.
33. Wayne PA. Clinical and Laboratory Standards Institute (CLSI). Performance standards for antimicrobial susceptibility testing. INFORM SUPPL. 2011;31:100-121.
34. Milani M, et al. Synthesis and evaluation of polymeric micelle containing piperacillin/tazobactam for enhanced antibacterial activity. Drug Deliv. 2019;26:1292-1299.
35. Tavakoli S, et al. Polydopamine coated ZnO rod-shaped nanoparticles with noticeable biocompatibility, hemostatic and antibacterial activity. Nano-Structures and Nano-Objects. 2021;25:100639.
36. Tavakoli S, et al. A multifunctional nanocomposite spray dressing of Kappa-carrageenan-polydopamine modified ZnO/L-glutamic acid for diabetic wounds. Mater Sci Eng C. 2020;111:110837.
37. Norouzzadeh P, et al. Comparative study on dielectric and structural properties of undoped, Mn-doped, and Ni-doped ZnO nanoparticles by impedance spectroscopy analysis. J Mater Sci Mater Electron. 2020;31:7335-7347.
38. Abdollahi B, et al. Fabrication of ZiF-8 metal organic framework (MOFs)-based CuO-ZnO photocatalyst with enhanced solar-light-driven property for degradation of organic dyes. Arab J Chem. 2021;14:103444.
39. Nie N, et al. Direct Z-scheme PDA-modified ZnO hierarchical microspheres with enhanced photocatalytic CO_2 reduction performance. Appl Surf Sci. 2018;457:1096-1102.
40. Lakshmi Prasanna V, et al. Insight into the Mechanism of Antibacterial Activity of ZnO: Surface Defects Mediated Reactive Oxygen Species even in the Dark. Langmuir. 2015;31:9155-9162.
41. Ahmed B, et al. Bacterial toxicity of biomimetic green zinc oxide nanoantibiotic: insights into ZnONP uptake and nanocolloid-bacteria interface. Toxicol Res (Camb). 2019;8:246-261.
42. Sirelkhatim A, et al. Review on zinc oxide nanoparticles: Antibacterial activity and toxicity mechanism. Nano-Micro Lett. 2015;7:219-242.
43. Morbach S, et al. Osmoregulation. Handbook of Corynebacterium Glutamicum.